Role of system size in freeze-out conditions extracted from transverse momentum spectra of hadrons

Ajay Kumar Dash,[1,*] Ranbir Singh,[1,†] Sandeep Chatterjee,[2,‡] Chitrasen Jena,[3,§] and Bedangadas Mohanty[1,‖]

[1]*School of Physical Sciences, National Institute of Science Education and Research, HBNI, Jatni 752050, India*

[2]*AGH University of Science and Technology, Faculty of Physics and Applied Computer Science, al. Mickiewicza 30, 30-059 Krakow, Poland and Department of Physical Sciences, Indian Institute of Science Education and Research, Berhampur, Transit Campus, Government ITI, Berhampur 760010, Odisha, India*

[3]*Indian Institute of Science Education and Research, Tirupati 517507, India*

(Received 13 July 2018; published 5 December 2018)

The data on hadron transverse momentum spectra in different centrality classes of p + Pb collisions at $\sqrt{s_{\rm NN}} =$ 5.02 TeV have been analyzed to extract the freeze-out hypersurface within a simultaneous chemical and kinetic freeze-out scenario. The freeze-out hypersurface has been extracted for three freeze-out schemes that differ in the way strangeness is treated: (i) unified freeze-out for all hadrons at complete thermal equilibrium (1FO), (ii) unified freeze-out for all hadrons with an additional parameter γ_S which accounts for possible out-of-equilibrium production of strangeness (1FO + γ_S), and (iii) separate freeze-out for hadrons with and without strangeness content (2FO). Unlike in heavy-ion collisions where 2FO performs best in describing the mean hadron yields as well as the transverse momentum spectra, with p + Pb we find that 1FO + γ_S with one fewer parameter than 2FO performs better. This confirms expectations based on previous analysis of system size dependence in the freeze-out scheme with mean hadron yields: while heavy-ion collisions that are dominated by constituent interactions prefer 2FO, smaller collision systems like proton + nucleus and proton + proton collisions with lesser constituent interaction prefer a unified freeze-out scheme with varying degrees of strangeness equilibration.

DOI: 10.1103/PhysRevC.98.064902

I. INTRODUCTION

Knowledge of the surface of last scattering of hadrons produced in a heavy-ion collision event is of utmost significance, as it contributes to the calibration of the hadronic physics baseline to be contrasted with data to extract information on the quark gluon plasma phase [1,2] as well as on the QCD critical point [3,4]. The hadron resonance gas model has been the main phenomenological model for extraction of the freeze-out hypersurface by comparison to the data on hadron yields [5–10] as well as spectra [11–14]. The surface where the hadrons cease to interact inelastically is known as the chemical freeze-out surface. The hadron yields freeze here. The surface where the hadrons cease to interact even elastically is known as the kinetic freeze-out surface. The shapes of the transverse momentum spectra of hadrons get fixed here. Depending on the model assumptions, the chemical and kinetic freeze-out surfaces can be separate [15–17] or together [11,12,18–20]. In this study, we have worked with the THERMINATOR event generator, where a combined freeze-out of both yields and spectra at the same surface is implemented [21,22].

Traditionally, a single unified freeze-out of all hadrons (1FO) has been studied [7–9]. However, data from the Large Hadron Collider (LHC) have thrown open the interpretation of freeze-out and several alternate schemes have been proposed [23–32]. In the standard picture, freeze-out is interpreted as a competition between fireball expansion and interaction of the constituents. Thus it is natural to expect system size dependence under freeze-out conditions, since constituent interactions decrease as one goes from nucleus-nucleus (A + A) to proton-nucleus (p + A) and proton-proton (p + p) collisions. On the contrary, it was found that 1FO provides an equally good description of the data on mean hadron yields of $e^+ + e^-$, p + p, and A + A [33]. This lack of sensitivity of the 1FO approach to the varying rate of interaction among the constituents and fireball expansion across system size raises doubt about the standard interpretation of freeze-out as a competition between expansion and interaction.

In Ref. [34], the yield data were analyzed within three approaches: (i) 1FO, (ii) single unified freeze-out of all hadrons with an additional parameter γ_S accounting for nonequilibrium production of strangeness (1FO + γ_S), and (iii) a separate freeze-out surface for hadrons with and without strangeness content (2FO). The data on hadron yield were analyzed across systems—p + p, p + Pb, and Pb + Pb—

*ajayd@niser.ac.in
†ranbir.singh@niser.ac.in
‡Sandeep.Chatterjee@fis.agh.edu.pl
§cjena@iisertirupati.ac.in
‖bedanga@niser.ac.in

Published by the American Physical Society under the terms of the Creative Commons Attribution 4.0 International license. Further distribution of this work must maintain attribution to the author(s) and the published article's title, journal citation, and DOI. Funded by SCOAP³.

enabling one to study the freeze-out condition for midrapidity charged particle multiplicity as well as the system volume varying over three orders of magnitude. It was found that while the 1FO and 1FO + γ_S schemes are blind to system size, 2FO exhibits a strong system size dependence. While for central and midcentral collisions, 2FO provides the lowest chi-square per degree of freedom, for peripheral Pb + Pb to all centralities of p + Pb and min bias p + p, 1FO + γ_S provides a better description. This emphasizes a plausible freeze-out scenario: in the case of large system sizes, the freeze-out dynamics is dominated by hadron interactions and hence flavor dependence in hadron-hadron cross sections plays a role, resulting in 2FO's being the preferred freeze-out scheme. On the other hand, in small systems the freeze-out is mostly driven by rapid expansion and little interaction, resulting in a sudden and rapid freeze-out and hence disfavoring 2FO.

In this paper, we extend the above line of argument by studying the data on hadron spectra. The 2FO prescription has been demonstrated to describe the data on hadron spectra better than 1FO in Pb + Pb at $\sqrt{s_{\rm NN}} = 2.76$ TeV [14]. Here we study the data on hadron spectra in p + Pb at $\sqrt{s_{\rm NN}} = 5.02$ TeV [35–37] and, finally, connect to our previous findings with the spectral data in Pb + Pb [14]. The spectra of $\pi^+ + \pi^-$, $\mathrm{K}^+ + \mathrm{K}^-$, $\mathrm{p} + \bar{\mathrm{p}}$, ϕ, $\Lambda + \bar{\Lambda}$, $\Xi + \bar{\Xi}$, and $\Omega + \bar{\Omega}$ are used for this study; they are measured in midrapidity ($0 < y_{\rm cm} < 0.5$) by the ALICE Collaboration. We have performed the centrality dependence in this study by analyzing the data in seven centrality classes: 0–5%, 5–10%, 10–20%, 20–40%, 40–60%, 60–80%, and 80–100%

The paper is arranged in the following way. In Sec. II we discuss the model used in this study. The results from the model and data are compared in Sec. III. Finally, we summarize our findings in Sec. IV.

II. MODEL

We have studied the data on hadron spectra in three schemes—1FO, 1FO + γ_S, and 2FO—using the THERMINATOR event generator [21,22]. While 1FO is implemented in the standard version of THERMINATOR, in Ref. [14] the standard version of THERMINATOR was extended to include the 2FO scheme. We now briefly describe the implementation of the freeze-out hypersurface and the relevant parameters to be extracted in this approach.

The Cooper-Frye prescription provides the hadron spectra emanating from a freeze-out hypersurface,

$$\frac{d^2N}{dy p_T dp_T} = \int d\Sigma \cdot p f(p \cdot u, T, \gamma_S, \mu), \tag{1}$$

where T is the temperature, $\mu = \{\mu_B, \mu_Q, \mu_S\}$ refer to the three chemical potentials corresponding to the three conserved charges of QCD, u^μ is the four-velocity, $d\Sigma^\mu$ is the differential element of the freeze-out hypersurface over which the integration in Eq. (1) is supposed to be, and p is the four-momentum. There can be different choices for parametrization of the freeze-out hypersurface and u^μ. We have worked within the Krakow model [11], whereby the freeze-out is assumed to occur at a constant proper time τ_f,

$$\tau_f^2 = t^2 - x^2 - y^2 - z^2, \tag{2}$$

while u^μ is chosen to be

$$u^\mu = x^\mu/\tau_f, \tag{3}$$

where (t, x, y, z) is the space-time coordinate.

THERMINATOR accounts for both primary production and the secondary contribution from resonance decays when evaluating the distribution function f. The integration in Eq. (1) occurs over the freeze-out hypersurface coordinates, namely, the space-time rapidity η_s, whose integration range is from $-\infty$ to $+\infty$; the azimuthal angle ϕ, which is integrated from 0 to 2π; and $\rho = \sqrt{x^2 + y^2}$, the perpendicular distance between the Z axis and the freeze-out hypersurface. ρ is integrated from 0 to $\rho_{\rm max}$. Thus, we have three parameters within the 1FO scheme—T, τ_f, and $\rho_{\rm max}$—to be extracted by comparison with data.

The choice of the thermodynamic ensemble is a relevant topic whenever one discusses system size dependence. In p + p collisions at the highest SPS and RHIC energies, the use of a canonical ensemble or a strangeness canonical ensemble has been suggested [38,39]. At the LHC energies, a grand canonical ensemble was found to work best in describing the hadron yields [40]. Similar recent studies on the role of the thermodynamic ensemble in small systems are reported in Refs. [41–43]. Here, we work with the grand canonical ensemble as well. Since we work with the LHC data, which shows a very good particle-antiparticle symmetry, we have set all the chemical potentials to 0. In 1FO + γ_S, there is also the additional parameter γ_S in f, which accounts for out-of-equilibrium production of strangeness. In 2FO, we have different parameter sets for parametrizing the nonstrange ($T_{\rm ns}$, $\tau_{f\,\rm ns}$, and $\rho_{\rm max\,ns}$) and strange ($T_{\rm s}$, $\tau_{f\,\rm s}$, and $\rho_{\rm max\,s}$) freeze-out hypersurfaces.

III. RESULTS

We have varied T in the range from 145 to 162 MeV in steps of 1–2 MeV, whereas $\rho_{\rm max}$ and τ_f are varied in the range 1.5 to 4.1 fm and 1.5 to 3.1 fm, respectively, in steps of 0.1 fm. The goodness of the parameter set in describing the data is ascertained from the χ^2/ndf, where

$$\chi^2 = \sum_i \left(\frac{\mathrm{Data}(p_{T\,i}) - \mathrm{Model}(p_{T\,i})}{\mathrm{Error}(p_{T\,i})} \right)^2, \tag{4}$$

and ndf = Number of data points – Number of free parameters. Here Error($p_{T\,i}$), the denominator, denotes the error in the experimental measurement, where the statistical and systematic errors have been added in quadratures.

The sum goes over all available p + Pb data points up to $p_T = 2.5$ GeV/c [35–37]. For 1FO, we have varied all three parameters, T, $\rho_{\rm max}$. and τ_f, to arrive at the best parameter set. In 1FO + γ_S, we have also varied γ_S in the range 0.7 to 1.0 in steps of 0.2, while in 2FO we have varied T, $\rho_{\rm max}$, and τ_f for both nonstrange and strange freeze-out hypersurfaces. The p_T spectra as obtained in the model for the different freeze-out schemes are compared with data in Fig. 1. In the bottom panel of Figs. 1(a)–1(i), we show the ratio of data to model. Unlike in Pb + Pb, where there is noticeable disagreement

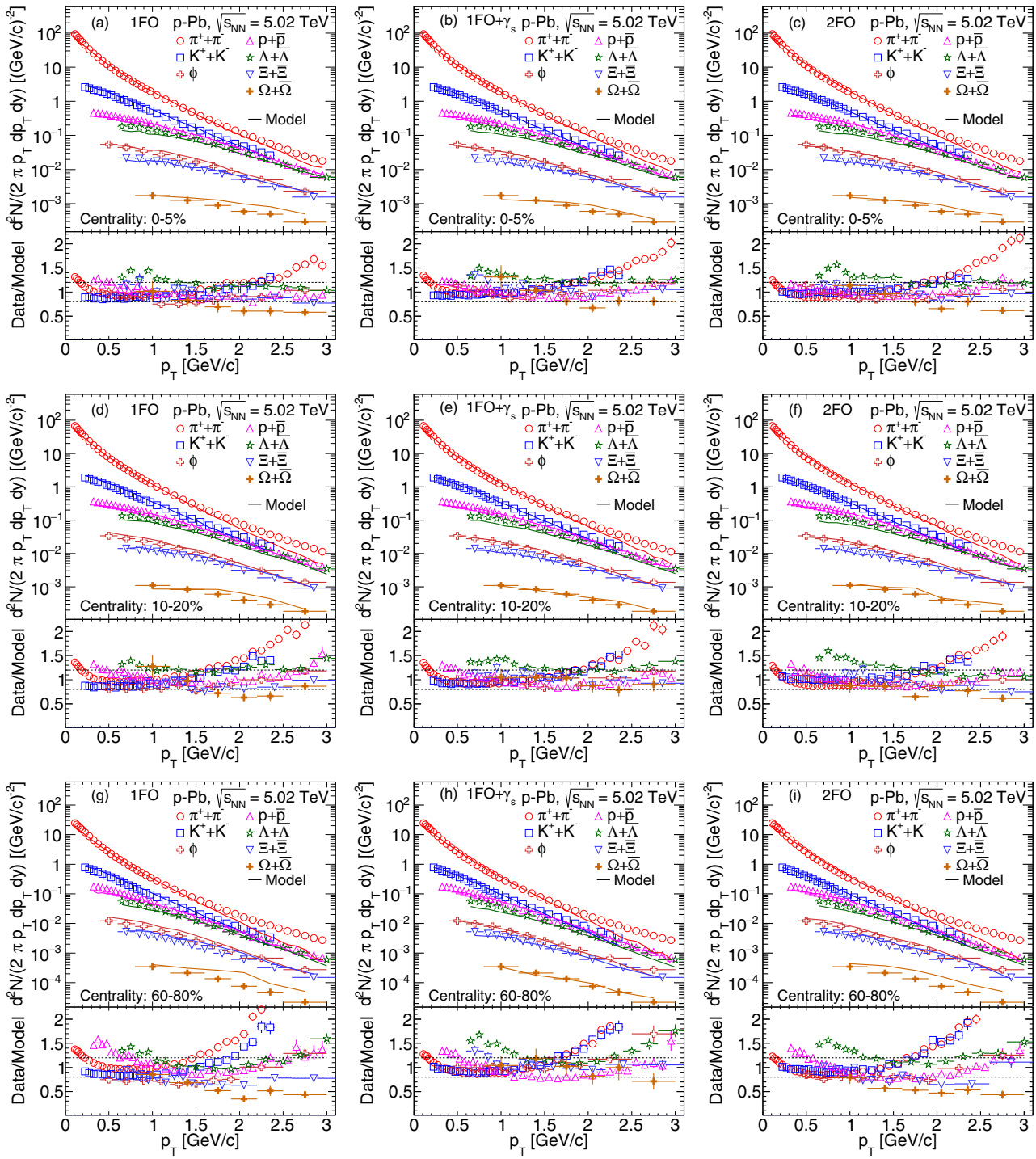

FIG. 1. Comparison of p_T spectra in p + Pb collisions at $\sqrt{s_{NN}} = 5.02$ TeV obtained from the THERMINATOR [21,22] and data [35–37] shown for three centralities—0-5%, 10–20%, and 60–80%—in three FO schemes at $0 < y_{cm} < 0.5$. The gross features of the spectral comparison seem to be independent of the freeze-out scheme. The bottom panels (a–i) show the ratio of data to model calculation.

between 1FO and data, referred to as a proton anomaly, which goes away upon extension of 1FO to 2FO, in p + Pb we do not find any such noteworthy tensions in 1FO. The quality of description of the spectra seems similar overall.

The χ^2/ndf values obtained in the different freeze-out schemes across various centralities are compared in Fig. 2 and the respective values of χ^2 and ndf are listed in Table I. For all centralities, 1FO + γ_S provides the lowest χ^2/ndf. The χ^2/ndf grows from around 3 in central collisions to around 10 in the most peripheral bin in this scheme. χ^2/ndf ~ 1 is the usual standard for a good statistical description. Thus, overall the χ^2/ndf obtained in our analysis is large. The occurrence of a large χ^2/ndf is quite common in these analyses [14,34,44] and this can be attributed to several factors. The uncertainties

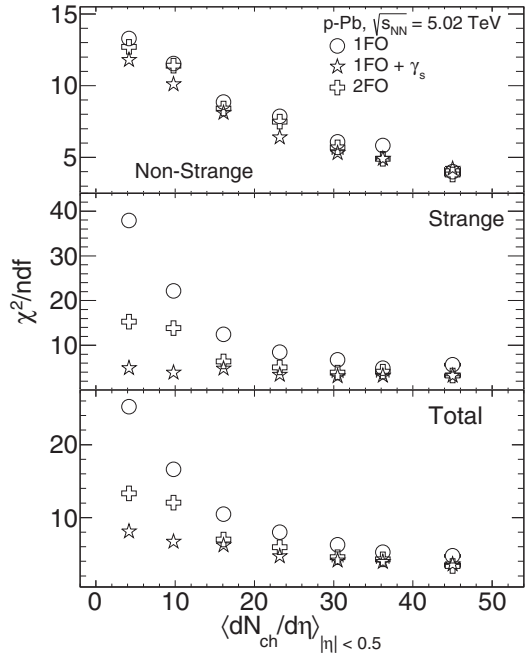

FIG. 2. The χ^2/ndf values are compared for the three freeze-out schemes across central to peripheral collisions in p + Pb. 1FO + γ_S provides the best description across all centralities. The improvement over 1FO and 2FO gets better as one goes to more peripheral collisions.

over the hadron spectrum [31,45–48], decay properties of hadrons [46,48,49], and treatment of hadron-hadron interaction [32,50–53] are some of the common sources of systematic improvements of such thermal models. It is usually found that accounting for such effects improves the quality of fits by lowering the χ^2/ndf substantially, keeping the extracted thermal parameters similar [32,48,49]. Further, one could also include corrections due to nonthermal physics such as the contribution from the rescattering phase post chemical freeze-out. So the assumption in this work is that even though such corrections will bring the χ^2/ndf down to within the admissible range of unity, the thermal physics of the freeze-out hypersurface that we extract here will not change under the incorporation of such systematic improvements of thermal as well as nonthermal effects.

The improvement of 1FO + γ_S over 1FO and 2FO increases as one goes from central to peripheral collisions. This is driven by the strange sector; it is more sensitive to the three freeze-out schemes studied here, which differ in the treatment of the freeze-out of strange hadrons. The yield in the nonstrange sector receives a partial contribution from the decays of strange resonances. This leads to a small sensitivity in the fit quality of the nonstrange sector to the different freeze-out schemes studied here. The improvement in the nonstrange sector with 1FO + γ_S is mild and uniform across centralities. We have enlisted the best parameter values that describe the transverse momentum spectra across different centralities within the three freeze-out schemes in Table II.

Finally, in Fig. 3 we have plotted the extracted freeze-out parameters corresponding to the lowest χ^2/ndf with event multiplicity across different centralities in p + Pb and Pb + Pb that vary over three orders of magnitude. While T remains mostly flat between 145 and 160 MeV, $\rho_{\max}$ and τ_f show an increase of 5–7 times. The growth rate is smooth across system size. We also note that the difference between nonstrange and strange freeze-out parameters systematically increase as we go to events with a higher multiplicity, signifying the role of interaction. However, currently the uncertainties over the extracted parameters in the nonstrange and strange sectors are large and do not allow us to further quantify the magnitude of the hierarchy in freeze-out of the strange and nonstrange flavors. γ_S in p + Pb steadily increases from 0.74 to about 0.94 across peripheral to central collisions. The approach to strangeness equilibration with more central p + Pb events could be related to the larger entropy deposition in the initial state in central p + Pb collisions as opposed to peripheral events [54]. We use similar errors in T, $\rho_{\max}$, and τ_f as for Pb + Pb results [14] since the errors are mostly system size independent.

IV. SUMMARY AND OUTLOOK

The hadron yields and p_T spectra are the standard observables to shed light on freeze-out dynamics. Contrary to expectations, the 1FO scheme is known to be blind to system size dependence in freeze-out [33]. However, simultaneous analysis of the hadron yields in Pb + Pb, p + Pb, and p + p revealed an interesting system size dependence of the

TABLE I. χ^2 and ndf in the 1FO, 1FO + γ_s, and 2FO schemes in p + Pb collisions at $\sqrt{s_{NN}} = 5.02$ TeV.

Centrality (%)	χ^2 (ndf)								
	1FO			1FO + γ_s			2FO		
	Nonstrange	Strange	Total	Nonstrange	Strange	Total	Nonstrange	Strange	Total
0–5	248 (62)	374(66)	622(131)	256(61)	208(65)	464(130)	225(59)	206(63)	432(128)
5–10	361(62)	325(66)	686(131)	297(61)	207(65)	504(130)	290(59)	257(63)	547(128)
10–20	377(62)	445(66)	822(131)	324(61)	204(65)	528(130)	338(59)	246(63)	584(128)
20–40	487(62)	560(66)	1046(131)	392(61)	219(65)	612(130)	441(59)	320(63)	761(128)
40–60	549(62)	822(66)	1371(131)	494(61)	315(65)	808(130)	495(59)	401(63)	896(128)
60–80	716(62)	1463(66)	2179(131)	615(61)	251(65)	866(130)	671(59)	873(63)	1544(128)
80–100	824(62)	2428(64)	3253(129)	721(61)	311(63)	1032(128)	746(59)	931(61)	1677(126)

TABLE II. Thermal freeze-out parameters in the 1FO, 1FO + γ_s, and 2FO schemes in p + Pb collisions at $\sqrt{s_{\rm NN}} = 5.02$ TeV. The average error in T and γ_s is 2 MeV and 0.02, respectively, whereas the error in $\rho_{\rm max}$ and τ_f is around 15% for all centrality classes.

Centrality (%)	1FO (1FO + γ_s)				2FO					
					Strange			Nonstrange		
	T (MeV)	$\rho_{\rm max}$ (fm)	τ_f (fm)	γ_s	T (MeV)	$\rho_{\rm max}$ (fm)	τ_f (fm)	T (MeV)	$\rho_{\rm max}$ (fm)	τ_f (fm)
0–5	157(158)	3.9(3.8)	2.7(2.7)	0.94	160	3.6	2.5	154	4.1	3.0
5–10	157(158)	3.5(3.5)	2.6(2.6)	0.92	160	3.3	2.3	154	3.8	2.8
10–20	157(157)	3.3(3.4)	2.5(2.5)	0.90	160	3.1	2.2	154	3.6	2.7
20–40	155(158)	3.1(3.0)	2.4(2.4)	0.88	158	2.8	2.2	152	3.3	2.7
40–60	155(156)	2.7(2.7)	2.2(2.3)	0.84	157	2.5	2.0	153	2.85	2.35
60–80	155(155)	2.2(2.3)	2.0(2.1)	0.80	156	2.1	1.9	153	2.4	2.2
80–100	154(153)	1.6(1.7)	1.9(1.9)	0.74	155	1.5	1.7	153	1.7	1.9

preferred freeze-out scheme: 2FO is preferred over 1FO and 1FO + γ_S in Pb + Pb, while in small systems like p + Pb and p + p, 1FO + γ_S is preferred [34]. In order to put this hypothesis on a stronger footing, here we extend the previous analysis to hadron spectra. While 2FO is known to describe the hadron spectra better in Pb + Pb, here we analyze the data for different centralities in p + Pb. We find that allowing for a different hypersurface for the freeze-out of the strange hadrons does not improve the quality of the fits. This is in accordance with our previous study of hadron yields [34]. Thus, our current analysis with the data on hadron spectra reaffirms the hypothesis on the system size dependence of the freeze-out scheme: a flavor-dependent freeze-out scheme is preferred in large systems, while unified freeze-out is preferred in small

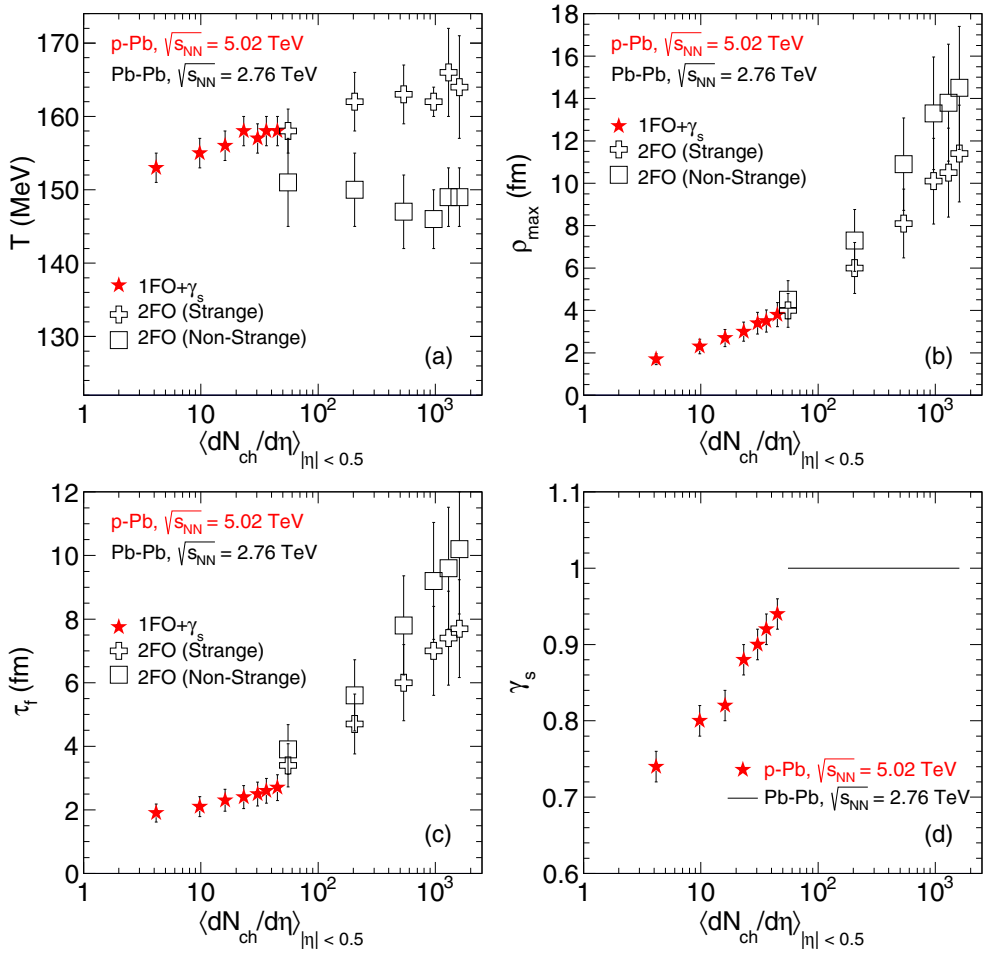

FIG. 3. The extracted freeze-out parameters with the best goodness of fit for different centralities in p + Pb and Pb + Pb collisions. There is a gradual preference for sequential freeze-out of the strange and nonstrange flavors as we go to higher multiplicity events. The γ_S value is fixed at 1 for Pb + Pb collisions at $\sqrt{s_{\rm NN}} = 2.76$ TeV.

systems. Thus, the role of interaction in larger systems is mostly to delay the freeze-out of nonstrange hadrons.

ACKNOWLEDGMENTS

A.K.D. and R.S. acknowledge the support of XIIth Plan Project No. 12-R&D-NIS-5.11-0300 of the Government of India. B.M. acknowledges financial support from the J. C. Bose National Fellowship of DST, Government of India. S.C. acknowledges the support of AGH UST statutory task No. 11.11.220.01/1 within the subsidy of the Ministry of Science and Higher Education and by National Science Centre Grant No. 2015/17/B/ST2/00101.

[1] M. Gyulassy and L. McLerran, Nucl. Phys. **A750**, 30 (2005).
[2] J. Adams *et al.* (STAR Collaboration), Nucl. Phys. **A757**, 102 (2005).
[3] K. Rajagopal and F. Wilczek, in *At the Frontier of Particle Physics*, edited by M. Shifman (World Scientific, Singapore, 2000), Vol. 3, pp. 2061–2151.
[4] M. A. Stephanov, Prog. Theor. Phys. Suppl. **153**, 139 (2004); *International Journal of Modern Physics A* (World Scientific, Singapore, 2005), Vol. 20, pp. 4387–4392.
[5] P. Braun-Munzinger, J. Stachel, J. P. Wessels, and N. Xu, Phys. Lett. **B365**, 1 (1996).
[6] G. D. Yen and M. I. Gorenstein, Phys. Rev. C **59**, 2788 (1999).
[7] J. Cleymans and K. Redlich, Phys. Rev. C **60**, 054908 (1999).
[8] F. Becattini, J. Cleymans, A. Keranen, E. Suhonen, and K. Redlich, Phys. Rev. C **64**, 024901 (2001).
[9] A. Andronic, P. Braun-Munzinger, and J. Stachel, Nucl. Phys. A **772**, 167 (2006).
[10] S. Chatterjee, S. Das, L. Kumar, D. Mishra, B. Mohanty, R. Sahoo, and N. Sharma, Adv. High Energy Phys. **2015**, 349013 (2015).
[11] W. Broniowski and W. Florkowski, Phys. Rev. Lett. **87**, 272302 (2001).
[12] W. Broniowski and W. Florkowski, Phys. Rev. C **65**, 064905 (2002).
[13] V. Begun, W. Florkowski, and M. Rybczynski, Phys. Rev. C **90**, 014906 (2014).
[14] S. Chatterjee, B. Mohanty, and R. Singh, Phys. Rev. C **92**, 024917 (2015).
[15] E. Schnedermann, J. Sollfrank, and U. W. Heinz, Phys. Rev. C **48**, 2462 (1993).
[16] M. van Leeuwen *et al.*, Nucl. Phys. A **715**, 161 (2003).
[17] J. M. Burward-Hoy (PHENIX Collaboration), Nucl. Phys. A **715**, 498 (2003).
[18] J. Letessier, J. Rafelski, and A. Tounsi, Phys. Lett. B **328**, 499 (1994).
[19] T. Csorgo and L. P. Csernai, Phys. Lett. B **333**, 494 (1994).
[20] L. P. Csernai and I. N. Mishustin, Phys. Rev. Lett. **74**, 5005 (1995).
[21] A. Kisiel, T. Taluc, W. Broniowski, and W. Florkowski, Comput. Phys. Commun. **174**, 669 (2006).
[22] M. Chojnacki, A. Kisiel, W. Florkowski, and W. Broniowski, Comput. Phys. Commun. **183**, 746 (2012).
[23] J. Steinheimer, J. Aichelin, and M. Bleicher, Phys. Rev. Lett. **110**, 042501 (2013).
[24] F. Becattini, M. Bleicher, T. Kollegger, T. Schuster, J. Steinheimer, and R. Stock, Phys. Rev. Lett. **111**, 082302 (2013).
[25] M. Petrán, J. Letessier, V. Petráček, and J. Rafelski, Phys. Rev. C **88**, 034907 (2013).
[26] R. Bellwied, S. Borsanyi, Z. Fodor, S. D. Katz, and C. Ratti, Phys. Rev. Lett. **111**, 202302 (2013).
[27] S. Chatterjee, R. M. Godbole, and S. Gupta, Phys. Lett. B **727**, 554 (2013).
[28] K. A. Bugaev, D. R. Oliinychenko, J. Cleymans, A. I. Ivanytskyi, I. N. Mishustin, E. G. Nikonov, and V. V. Sagun, Europhys. Lett. **104**, 22002 (2013).
[29] M. Floris, Nucl. Phys. A **931**, 103 (2014).
[30] J. Noronha-Hostler and C. Greiner, Nucl. Phys. **A931**, 1108 (2014).
[31] A. Bazavov, H. T. Ding, P. Hegde, O. Kaczmarek, F. Karsch, E. Laermann, Y. Maezawa, S. Mukherjee, H. Ohno, P. Petreczky, C. Schmidt, S. Sharma, W. Soeldner, and M. Wagner, Phys. Rev. Lett. **113**, 072001 (2014).
[32] P. Alba, V. Vovchenko, M. I. Gorenstein, and H. Stoecker, Nucl. Phys. A **974**, 22 (2018).
[33] F. Becattini, P. Castorina, A. Milov, and H. Satz, Eur. Phys. J. C **66**, 377 (2010).
[34] S. Chatterjee, A. K. Dash, and B. Mohanty, J. Phys. G **44**, 105106 (2017).
[35] B. B. Abelev *et al.* (ALICE Collaboration), Phys. Lett. B **728**, 25 (2014).
[36] J. Adam *et al.* (ALICE Collaboration), Phys. Lett. B **758**, 389 (2016).
[37] J. Adam *et al.* (ALICE Collaboration), Eur. Phys. J. C **76**, 245 (2016).
[38] I. Kraus, J. Cleymans, H. Oeschler, K. Redlich, and S. Wheaton, Phys. Rev. C **76**, 064903 (2007).
[39] I. Kraus, J. Cleymans, H. Oeschler, and K. Redlich, Phys. Rev. C **79**, 014901 (2009).
[40] S. Das, D. Mishra, S. Chatterjee, and B. Mohanty, Phys. Rev. C **95**, 014912 (2017).
[41] V. V. Begun, V. Vovchenko, M. I. Gorenstein, and H. Stoecker, arXiv:1805.01901.
[42] N. Sharma, J. Cleymans, and L. Kumar, Eur. Phys. J. C **78**, 288 (2018).
[43] N. Sharma, J. Cleymans, and B. Hippolyte, arXiv:1803.05409.
[44] V. Begun, W. Florkowski, and M. Rybczynski, Phys. Rev. C **90**, 054912 (2014).
[45] W. Broniowski and W. Florkowski, Phys. Lett. B **490**, 223 (2000).
[46] S. Chatterjee, R. M. Godbole, and S. Gupta, Phys. Rev. C **81**, 044907 (2010).
[47] P. Alba, R. Bellwied, S. Borsányi, Z. Fodor, J. Günther, S. D. Katz, V. Mantovani Sarti, J. Noronha-Hostler, P. Parotto, A. Pasztor, I. P. Vazquez, and C. Ratti, Phys. Rev. D **96**, 034517 (2017).
[48] S. Chatterjee, D. Mishra, B. Mohanty, and S. Samanta, Phys. Rev. C **96**, 054907 (2017).
[49] V. Vovchenko, M. I. Gorenstein, and H. Stoecker, Phys. Rev. C **98**, 034906 (2018).
[50] V. Vovchenko, A. Pasztor, Z. Fodor, S. D. Katz, and H. Stoecker, Phys. Lett. B **775**, 71 (2017).

[51] V. Vovchenko, M. I. Gorenstein, and H. Stoecker, Phys. Rev. Lett. **118**, 182301 (2017).
[52] P. Huovinen and P. Petreczky, Phys. Lett. B **777**, 125 (2018).
[53] A. Dash, S. Samanta, and B. Mohanty, Phys. Rev. C **97**, 055208 (2018).
[54] P. Castorina, S. Plumari, and H. Satz, Intl. J. Mod. Phys. E **26**, 1750081 (2017).